

A Study on Maximum Power Point Tracking for Wind Power Generations

Doan Kim Tuan

Electrical Faculty, Thai Nguyen University of Technology, Thai Nguyen, Vietnam

DOI: <https://doi.org/10.52403/ijrr.20231158>

ABSTRACT

This paper presents a study on maximum power point tracking for a wind turbine generation (WTG). The general structure of a WTG will be introduced, including mechanical and electrical conversion blocks, to make clear about the role of all units. Moreover, mathematical models of both turbine and generator type permanent magnet synchronous generator (PMSG) will be presented to simulate and evaluate the operation of WTG. Working regions of the wind turbine corresponding to different values of wind speed and contents of some techniques to determine maximum power point will be made detailed. Hill climb search (HCS) is chosen to simulate and analyzed deeply to evaluate the ability to apply to real applications. Simulation results are carried out by MATLAB/Simulink software. By using a variation scenario of wind speed, the role of power converter and HCS controller will be presented in some simulation results about power and current at output terminals of the generator to show the ability to track instantaneous maximum power point. Research results show the high effectiveness and availability of HCS technique in real wind power system.

Keywords: Maximum power point, Maximum power point tracking, Wind turbine, Wind generator, Wind speed, PMSG.

I. INTRODUCTION

Wind turbine generation (WTG) is one of the most popular generations in modern power system. WTGs can be installed both onshore and offshore areas. Their implemented capacity increases very much every year. Moreover, they were designed and classified into many types of turbines

and generators and have been interested in recently [1-2].

Popular turbines are designed in vertical or horizontal axis, where horizontal axis turbines are more popular than vertical axis turbines. A wind generator can be specified by rated voltage and power, and its structure. Almost wind generators generate three-phase currents same as normal generators. Their rated voltage is in complete proportion to designed power. Classified by structure, wind generators includes Asynchronous Generator (ASG) and Synchronous Generator (SG). For above classification, Double Fed Asynchronous Generator (DFIG) and Permanent Magnet Generator (PMSG) are the most popular wind generators in the world [1-2]. PMSG can be used wider than DFIG due to simple design, operation and control. So, PMSG will be chosen to study deeply in this paper.

Each turbine is designed in an optimal operating speed. When wind speed changes, system of turbine blades must be controlled by using mechanical units to regulate pit and yaw angles that change the stall phenomenon or automatic stopping rotation to ensure safety. In cases of low wind speed, system of turbine blades must be controlled to have more sectional area that helps to extract more power. In cases of high wind speed, system of turbine blades must be controlled to reduce rotating speed [1]. This mechanical system can help to improve apart but it make small energy efficiency.

In the other approach, WTG always has an operating state that extract its maximum power. To harness this power, the absorbability of load must be regulated

equally to power at maximum power point (MPP) corresponding to natural operating conditions. They include pit angle, air density, wind speed, etc. Designing power converters and controllers to harness power at MPP was proposed by many researchers is the best solution for WTG. In this solution, electric loads must have enough capability to absorb all power at MPP, so they are often energy storage (ES) or utility (power system). Power converters are used to regulate load consumption that affects to the speed rotation of the turbine by using Maximum Power Point Tracker (MPPT). To track MPP continuously, many different techniques have been proposed to apply in MPPT. The simplest technique uses current signal. Currents at output terminals of the generator are compared with reference current determined by speed turbine. This technique creates large fluctuation. Tip Speed Ratio (TSR) and Power Signal Feedback (PSF) are popular techniques in WTG system but they must use speed and wind sensors. Incremental conductance (INC) and Hill Climb Search (HSC) techniques collect information about voltage and current at output terminals of the generator to determine the location of operating point and MPP [1], [3-18]. Recently, some advanced techniques have been proposed in WTG system based on intelligent techniques such as artificial neural networks (ANN) or fuzzy logic (FL) but they have high requirements for control and device.

From above analysis, it needs to have more researches to evaluate the ability to harness power from WTG using power converters corresponding to different values of wind speed. The next section will introduce mathematical models of both horizontal turbine and generator type PMSG. The third section will analyze working regions of the turbine and make clear about some techniques that can help to harness power at MPP. The fourth section will present some simulation results for a 8,5 kW rated generator type PMSG in a wind speed variation. The last section will show some conclusions and contributions of this paper.

II. Mathematical Model Of Wtg

A. General structure of WTG

Systems of turbine and generator convert wind energy to mechanical energy on turbine axis. The general structure of this system is depicted in Fig.1 [1-3], [12], [16].

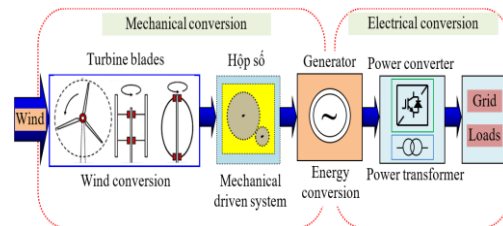


Fig.1 General structure for WTG

Turbine blades are designed in horizontal or vertical axis types to convert wind kinetic energy to rotating movements on turbine axis. They must be designed to stand high wind speed, sudden change of wind direction or many different harsh operating conditions.

The gearbox is coupled to turbine and generator axis. It converts low speed of turbine axis (about (30÷60) round/min) to high speed of generator axis (about (1200÷1500) round/min).

The generator converts magnetic rotating field on generator axis to electric energy.

Power converters and transformers help to regulate working modes for the generator, step up voltage and synchronize to the grid.

B. Mathematical model of wind turbine

Turbine blades only convert apart energy of wind energy to mechanical energy on turbine axis, called P_m . Value of P_m can be determined by equation (1) [8-9]:

$$C_p = \frac{P_m}{P_w} \quad (1)$$

where: P_w is instantaneous wind power; C_p is a function of tip speed ratio λ (or called TSR) and pitch angle β .

Function of C_p can be determined by manufacturers for each type of turbine as equation (2) [8-9]:

$$C_p(\lambda, \beta) = c_1 \left(\frac{c_2}{\lambda_i} - c_3 \beta - c_4 \right) e^{-\frac{c_5}{\lambda_i}} + c_6 \lambda \quad (2)$$

where: $c_1, c_2, c_3, c_4, c_5, c_6$ are constants; λ_i is function of TSR and β ; $\lambda = \frac{\omega_{\text{turbine}} R}{v_w}$; ω_{turbine} is turbine speed, R is radial of turbine blades.

For each value of β , it always has an optimal value, called λ_{op} that provide C_{pmax} and P_{mpp} .

Mechanical moment T_m can be determined by equation (3) [8]:

$$T_m = \frac{P_m}{\omega_{\text{turbine}}} \quad (3)$$

The relationship between electrical moment T_e , mechanical moment T_m and ω_{turbine} is defined by equation (4) [8-9]:

$$T_m - T_e = J \frac{d}{dt} \omega_{\text{turbine}} + D_p \omega_{\text{turbine}} \quad (4)$$

where: J is inertia constant (kgm^2) and D_p is damping factor.

C. Mathematical model of generator type PMSG

Mathematical model of PMSG can be described by establishing dq rotational axis from equations in three-phase system to dq0 axis. This axis can help to dispose of inductance variation by using stator and rotor quantities. Using Park's transform, we have equation (5) [8-9]:

$$\begin{cases} V_d = \frac{2}{3} \left[V_a \sin(\omega t) + V_b \sin\left(\omega t - \frac{2\pi}{3}\right) + V_c \sin\left(\omega t + \frac{2\pi}{3}\right) \right] \\ V_q = \frac{2}{3} \left[V_a \cos(\omega t) + V_b \cos\left(\omega t - \frac{2\pi}{3}\right) + V_c \cos\left(\omega t + \frac{2\pi}{3}\right) \right] \\ V_0 = \frac{1}{3} (V_a + V_b + V_c) \end{cases} \quad (5)$$

where, ω is rotational speed on the axis.

I_d, I_q, I_0 current quantities are also transformed same as voltage quantities.

For PMSG, magnetic flux is created in direction of d axis. Stator voltage equations can be described by equations (6) and (7) [8-9]:

$$V_d^s = -R_s i_d^s - \omega_e \lambda_q^s + \frac{d}{dt} \lambda_d^s \quad (6)$$

$$V_q^s = -R_s i_q^s + \omega_e \lambda_d^s + \frac{d}{dt} \lambda_q^s \quad (7)$$

Leak magnetic flux can be determined by equations (8) and (9) [8-9]:

$$\lambda_d^s = -L_d i_d^s + \Psi \quad (8)$$

$$\lambda_q^s = -L_q i_q^s \quad (9)$$

where: V_d^s and V_q^s are stator voltage on d-q axis; i_d^s and i_q^s are stator current on d-q axis; λ_d^s and λ_q^s are stator leak magnetic flux on d-q axis; ω_e is electrical speed of rotor; R_s is resistance of stator winding; Ψ is flux of permanent magnetic created by rotor.

Replacing equations (8) and (9) into equations (6) and (7), we have voltage equations (10) and (11) [8-9]:

$$V_d^s = -R_s i_d^s + \omega_e L_q i_q^s - L_d \frac{d}{dt} i_d^s \quad (10)$$

$$V_q^s = -R_s i_q^s + \omega_e L_d i_d^s + \omega_e \Psi - L_q \frac{d}{dt} i_q^s \quad (11)$$

Equivalent circuit of PMSG based on equations (10) and (11) is depicted in Fig. 2 [8-9].

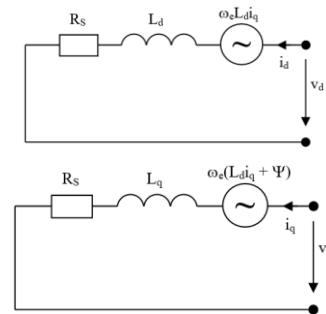


Fig.2 Equivalent circuit of PMSG

Electrical moment can be determined by equation (12) [8-9]:

$$T_e = \frac{3}{2} p \left[\Psi i_q^s - (L_d - L_q) i_d^s i_q^s \right] \quad (12)$$

where: L_q is inductance on q axis; R is resistance of stator winding; i_q is current on q axis; i_d is current on d axis; v_q is voltage on q axis; v_d is voltage on d axis; ω_r is rotational speed of rotor; p is the number pair of poles.

In a PMSG, magnetic flux created by a magnet is constant and can be supposed in d axis. So, λ_q^s quantity in electrical moment

equation can be ignored. Moreover, inductance quantities in d axis and q axis have the same value ($L_d=L_q$). Due to this reason, equation (8) can be converted to equation (13) [8-9]:

$$T_e = \frac{3p}{2} \Psi i_q^s \quad (13)$$

Current quantities on d-q axis can be determined by equations (14) and (15) [8-9]:

$$i_d^s = \frac{1}{s} (-V_d^s - R_s i_d^s + \omega_e L_q i_q^s) / L_d \quad (14)$$

$$i_q^s = \frac{1}{s} (-V_q^s - R_s i_q^s - \omega_e L_d i_d^s + \omega_e \Psi) / L_q \quad (15)$$

Power at output terminals of PMSG can be determined by equation (16) [8-9]:

$$P_g = P_m - P_{loss} = T_e \frac{\omega_e}{p} - R_s I_s^2 \quad (16)$$

where: $I_s = \sqrt{i_d^s{}^2 + i_q^s{}^2}$

III. Maximum power point tracking techniques

A. Working regions of a wind turbine

Working regions of a wind turbine can be divided into 4 parts as described in Fig. 3 [1], [16].

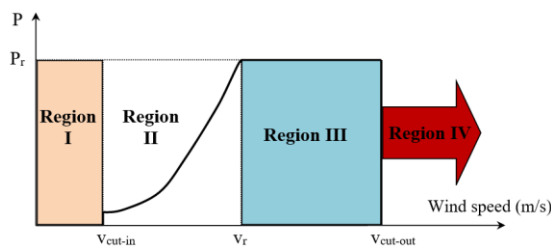


Fig. 3 Working regions of a wind turbine

where: v_{cut-in} is cut-in speed; $v_{cut-out}$ is cut-out speed; v_r is rated speed; P_r is rated power.

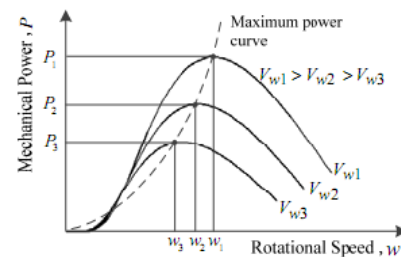
Region I ($v_w < v_{cut-in}$) or Region IV ($v_w > v_{cut-out}$): generator does not generate power, where v_w is wind speed. In Region I, turbine rotates too slowly and does not create enough magnetic field. In Region IV, turbine must be cut out to protect mechanical units.

Region II ($v_{cut-in} \leq v_w < v_r$): PMSG can generate power but it is always smaller than rated power.

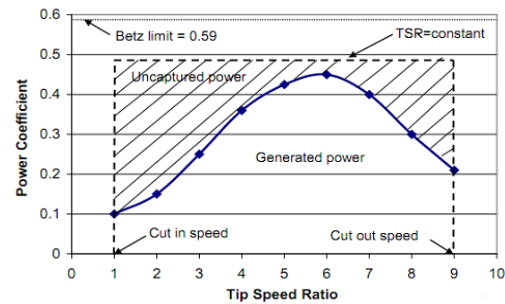
Region III ($v_r \leq v_w < v_{cut-out}$): the generator can generate rated power.

B. TSR technique to track MPP

TSR technique determines MPP by evaluating values of wind speed in $P(\omega)$ curves. These curves must be created by simulation or experiment for each turbine. Value of optimal TSR_{opt} at any working condition will help to extract maximum power from WTG as depicted in Fig. 4 [7], [16].



a. $P(\omega)$ curves and the orbit of MPP



b. $P(TSR)$ curve

Fig. 4 $P(\omega)$ and $P(TSR)$ curves

To use this method, wind speed must be measured continuously to track MPP in real time. So, the cost for whole system using small rated power increases. Based on TSR_{opt} , optimal speed for the turbine can be determined by (18) [7]:

$$\omega_{opt} = \frac{TSR_{opt} v_w}{R} \quad (18)$$

where: R is the radius of the circle swept by blades of the turbine.

The controller will compare ω_{opt} and current value of ω to determine suitable control

pulse and regulate power converters as depicted in Fig. 5 [7].

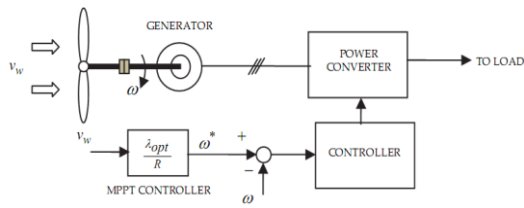


Fig. 5 TSR control method

This method cannot help to harness maximum power because of the fast change of wind speed and the inertia of wind turbine and generator.

C. PSF method

To execute PSF method, MPP can be tracked by measuring the speed at the shaft of the turbine and using the orbit of power reference. This orbit is also provide by manufacturers.

The controller will compare P_{opt} and current value of P to determine suitable control pulse and regulate power converters as depicted in Fig. 6 [16].

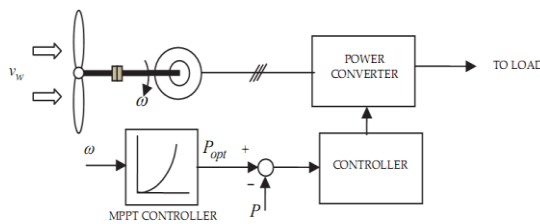


Fig. 6 PSF method

D. HCS method

HCS method always determines peak power of the turbine by "searching - remembering - recording" process. It can help to overcome some disadvantages of above method by tracking the operating points and the relation of power and speed. This process calculates values of power in the past and the current operating point will be determined at uphill or downhill as depicted in Fig. 7 [7], [13], [16].

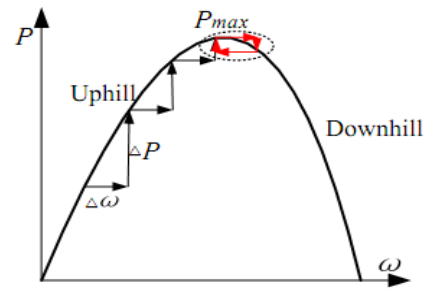


Fig. 7 Principle of HCS method

MPP at each wind speed can be determined by the following relationship:

If $\frac{dP}{d\omega} > 0$ or $\frac{\Delta P(k)}{\Delta \omega(k)} > 0$, the rotating speed ω

$< \omega_{MPP}$

$\frac{dP}{d\omega} = 0$ or $\frac{\Delta P(k)}{\Delta \omega(k)} = 0$, the rotating speed $\omega =$

ω_{MPP}

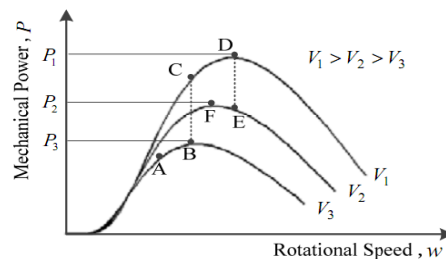
$\frac{dP}{d\omega} < 0$ or $\frac{\Delta P(k)}{\Delta \omega(k)} < 0$, the rotating speed $\omega >$

ω_{MPP}

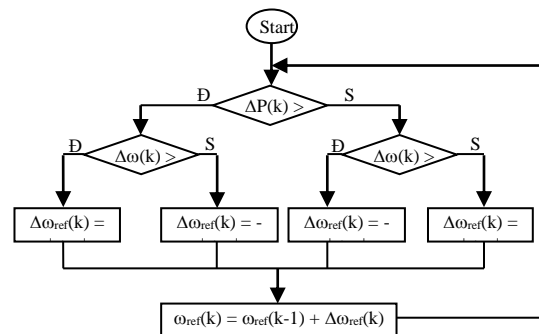
where: $\Delta P(k) = P(k) - P(k-1)$,

$\Delta \omega(k) = \omega(k) - \omega(k-1)$.

The control algorithm of HCS method is represented in Fig. 8.



a. The change of operating points at different wind speeds



b. Control algorithm

Fig. 8 HCS control method to determine MPP

Supposing that the turbine is operated at point B as shown in Fig. 8a. The wind speed increases and point B will be moved to point C corresponding to new values of mechanical power and rotational speed of the turbine. The controller must be created a suitable control pulse to increase the rotational speed of the turbine that help to move point C to point D (new MPP). The controller collects the information about current and voltage values at output terminals of the generator to determine mechanical power. The speed sensor is used to measure instantaneous speed of the turbine. The value of step in Fig. 8b can be adjusted to have a fast response of the turbine and the convergence speed of the algorithm. If it is too high, it can affect much to the power fluctuation and loss in power converters.

IV. Simulation Results

A WTG is regulated by a rectifier (without controlling) and a DC/DC buck power converter with parameters in TABLE I.

Simulation parameters of a WTG is shown in TABL I.

Table I Parameters of Power Converter

Number	Name of parameter	Symbol	Value
1	Inductance	L	8×10^{-4} H
2	Capacitance	C	2×10^{-4}
3	Switching frequency	f_{sw}	50 kHz
4	Voltage at DCbus	V_{dc}	400

Table II. Parameters of WTG

Number	Name of parameter	Symbol	Value
1	Rated power	P_r (W)	8500
2	Rated wind speed	v_r (m/s)	12
3	Radius	R (m)	5
4	Resistance of stator winding	R_s (Ω)	1.2
5	Equivalent inductance of stator winding on d axis	L_d (H)	0.066
6	Equivalent inductance of stator winding on q axis	L_q (H)	0.066
7	Self inductance	L_σ (H)	0.066
8	Magnetic flux of the rotor	Flux (Weber)	1.546
9	Inertia of rotor and turbine	J (kgm^2)	0.12
10	Damping factor of rotor	D_p	0.005

C_p function can be determined by (19) [13], [18]:

$$C_p(\lambda, \beta) = 0.5176 \left(\frac{116}{\lambda_i} - 0.4\beta - 5 \right) e^{-\frac{21}{\lambda_i}} + 0.0068\lambda \quad (19)$$

where: $\frac{1}{\lambda_i} = \frac{1}{\lambda + 0.08\beta} - \frac{0.035}{1 + \beta^3}$

Based on $C_p(\lambda, \beta)$ function, the $P(\lambda, v_w)$ curves are represented in Fig. 9. It is easy to show that P_{mpp1} is the largest power value (corresponding to 8.5 kW-rated power at 12 m/s-wind speed). In cases of decreasing wind speed to 10 m/s, 8 m/s, 6 m/s, $P(\lambda, v_w)$ curves become lower than it at 12 m/s wind speed, so peak power at these curves is also smaller than rated power. It means that the operation of the turbine can be correctly neglected in real working process by using the mathematical model of $C_p(\lambda, \beta)$ function.

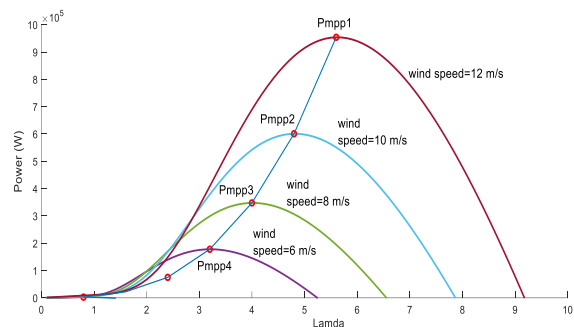


Fig. 9 $P(\lambda, v_w)$ curves of simulated turbine

A scenario is considered as depicted in Fig. 10. There are three time ranges that values of wind speed are constants, including $(0.4 \div 1)$ s, $(1.8 \div 3)$ s, and $(6 \div 7)$ s. There are two time ranges that wind speed increases, including $(1 \div 1.8)$ s and $(4.5 \div 6)$ s. In time range $(3 \div 4.5)$ s, wind speed decreases slowly and suddenly reduce from 10.5 m/s to 8.5 m/s at 4.5 s. This scenario describes the variation of wind speed in natural operating conditions.

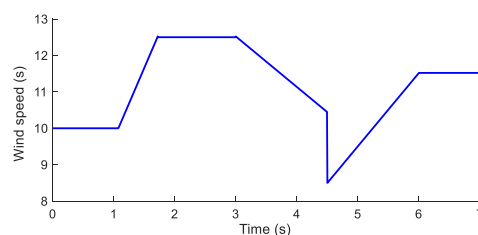


Fig.10 Variation of wind speed

Simulation result about current at output terminals of phase A from the generator in whole considered time range is represented in Fig. 11. Magnitude of the current increased or decreased same as the variation of wind speed variation.

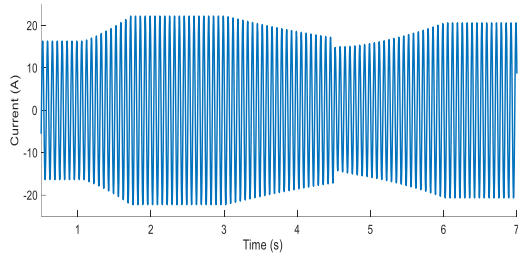


Fig.11 Current at output terminals of phase A in whole considered time range

Considering in a specific timer range (1÷2) s, current in phase A has pure sine waveform as depicted in Fig. 12. It showed the accuracy of controller to regulate the generator.

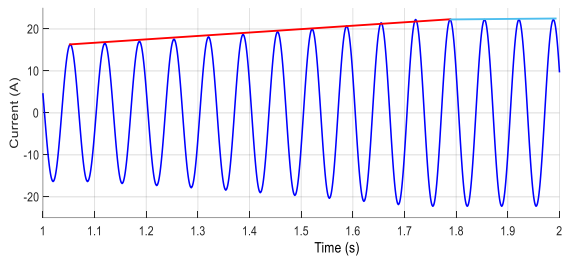


Fig. 12 Current in phase A in time range (1÷2) s

Simulation result about power from WTG in whole considered time range is depicted in Fig. 13. Value of power reached to maximum power corresponding to rated power in time range (1.8÷3) s and was held a constant value due to constant wind speed. If wind speed is smaller than 12 m/s and constant, power from the generator was also held at constant values but they were smaller than rated power. Moreover, power from WTG also increased or decreased corresponding same as the variation of wind speed. It means that the mathematical model of WTG and controller were designed correctly to completely neglect the response of WTG in all cases with the variation of wind speed values.

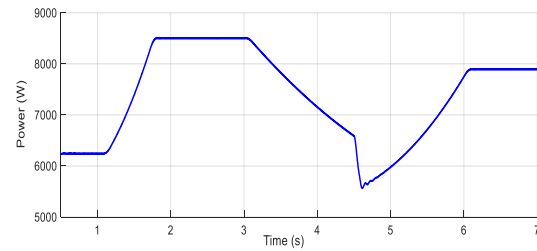


Fig. 13 The variation of power from WTG

V. CONCLUSIONS

Successful simulation for a 8.5 kW rated power is the main science contribution of this paper to have evaluations before installing WTG in real systems. This paper also introduced the general structure for a wind system, mathematical model for a turbine and a generator type PMSG, characteristics for a WTG, and three control methods applied in wind system, including TSR, PSF, and HCS methods. Simulation results were carried out by MATLAB/Simulink software using achieved mathematical models and HCS method.

From simulation results, the paper proved the only one peak power at a wind speed value. A new MPP will appears in cases of having a new value of wind speed. In a specific variation of wind speed, HCS controller helped to track MPP correctly and power from WTG is always maximum. The simulation results showed that WTG only generated rated power if values of wind speed are higher than rated value (12 m/s). Furthermore, power from WTG is always smaller than rated power and has classical proportions of wind speed. It represented the high accuracy of mathematical models, control design and simulation for whole system. The high response of the controller help to evaluate the operation of WTG in different working conditions.

Research results of the paper can be applied in real applications of isolated grid with the participation of energy storage systems or grids that can absorb all power from MPP. In cases of using small rated power for PMSG, they are also used to apply in a hybrid

system with the participation of both WTG and photovoltaic power generations. This hybrid system can be operated in half-isolated operating mode which exchanges power in bidirections between generation side and grid side at some time ranges to dispatch whole power system. This proposed idea can help to reduce disadvantages of renewable power generations and problem of inertia system due to their fast response.

Declaration by Authors

Acknowledgement: This study is completely supported by Thai Nguyen University of Technology, Thai Nguyen University, Viet Nam.

Source of Funding: None

Conflict of Interest: The authors declare no conflict of interest.

REFERENCES

1. Le Tien Phong, Duong Hoa An, Ngo Duc Minh, Vu Xuan Tung, *Design and Integration of Renewable Energy Systems*, A Book published in Publisher of Thai Nguyen University, 2021.
2. Teresa Orłowska-Kowalska, Frede Blaabjerg, José Rodríguez (2014), "Advanced and Intelligent Control in Power Electronics and Drives", *Springer Publisher*, Volume 531, ISBN 978-3-319-03401-0.
3. Devbratta Thakur, *Power Management Strategies for a Wind Energy Source in an Isolated Microgrid and Grid Connected System*, Thesis submitted in partial fulfillment of the requirements for the degree in Doctor of Philosophy, University of Western Ontario, 2015.
4. Jeremy Dulout, Amjad Anvari-Moghaddam, Adriana Luna, Bruno Jammes, Corinne Alonso, Josep Guerrero, *Optimal sizing of a lithium battery energy storage system for grid-connected photovoltaic systems*, IEEE Second International Conference on DC Microgrids (ICDCM), 2017, ISBN: 978-1-5090-4479-5.
5. Nabeel Ahmad, *Hybrid power system With Smart Energy Management System*, Proceedings of the 2nd International Conference on Engineering & Emerging Technologies (ICEET), 2015.
6. Jiyong Li, Honghua Wang, Maximum Power Point Tracking of Photovoltaic Generation Based on the Optimal Gradient Method, Power and Energy Engineering Conference, IEEE, 2009, Print ISSN: 2157-4839, Electronic ISSN: 2157-4847
7. Shrikant S Mali, B. E. Kushare, *MPPT Algorithms: Extracting Maximum Power from Wind Turbines*, International Journal of Innovative Research in Electrical, Electronics, Instrumentation and Control Engineering, ISSN (Online) 2321 – 2004, ISSN (Print) 2321 – 5526, 2013, Vol. 1, Issue. 5.
8. S. Samanvorakij, P. Kumkratug, *Modeling and Simulation PMSG based on Wind Energy Conversion System in MATLAB/SIMULINK*, Conference on Advances in Electronics and Electrical Engineering (AEEE), ISBN: 978-981-07-5939-1, 2013.
9. A.Bharathi Sankar, R.Seyezhai, *MATLAB Simulation of Power Electronic Converter for PMSG Based Wind Energy Conversion System*, International Journal of Innovative Research in Electrical, Electronics, Instrumentation and Control Engineering, 2013, Vol. 1, Issue 8.
10. M . Mahdi Mansouri1, M. Hosein Shafiei, Majid Nayeripour (), *A New Maximum Peak Power Tracking Method Improvement in the Wind Energy Conversion Systems Using Optimal Control*, Global Journal of Advanced Engineering Technologies, ISSN: 2277-6370, 2013, Vol. 2, Issue. 4.
11. Jin Yang, *Fault Analysis and Protection for Wind Power Generation Systems*, Dissertation for the degree of Doctor of Philosophy (Ph.D.) in University of Glasgow, 2011.
12. Johel Rodríguez D'Derlée, *Control strategies for offshore wind farms based on PMSG wind turbines and HVDC connection with uncontrolled rectifier*, Dissertation for the degree of Doctor of Philosophy (Ph.D.) in University Polytechnique of Valencia, 2013
13. M . Mahdi Mansouri1, M. Hosein Shafiei, Majid Nayeripour (), *A New Maximum Peak Power Tracking Method Improvement in the Wind Energy Conversion Systems Using Optimal Control*, Global Journal of Advanced Engineering Technologies, ISSN: 2277-6370, 2013, Vol. 2, Issue. 4.

14. Manish Kumar Yadav and Amrish Kumar Upadhayay, Power Flow Control of Permanent Magnet Synchronous Generator Based Wind Energy Conversion System with DC-DC Converter and Voltage Source Inverter, *International Journal of Electronic and Electrical Engineering*, ISSN 0974-2174, 2014, Volume 7, Number 8, pp. 803-814.
15. Lucky Dube Dube, Graham C. Garner, Karen S. Garner and Maaren J. Kamper, *Simple and Robust MPPT Current Control of a Wound Rotor Synchronous Wind Generator*, *Energies* 2023, 16(7).
16. Jayshree Pande, Paresh Nasikkar, Ketan Kotecha and Vijayakumar Varadarajan, *A Review of Maximum Power Point Tracking Algorithms for Wind Energy Conversion Systems*, *Journal of Marine Science and Engineering*, 9, 1187, 2021.
17. F Ronilaya, B Setiawan, A A Kusuma, I Mahfudi and D M Yuliawan, *Design Maximum Power Point Tracking of Wind Energy Conversion Systems Using P&O and IC Methods*, *IOP Conference Series: Materials Science and Engineering*, 407, 01259, 2018.
18. K. Ishwarya, Dr. K. Yasoda, *Maximum Power Point Tracking in Solar and Wind Hybrid Energy Conversion System*, *International Journal for Modern Trends in Science and Technology*, ISSN: 2455-3778, Vol. 6, Issue 7, 2020.

How to cite this article: Doan Kim Tuan. A Study on Maximum Power Point Tracking for Wind Power Generations. *International Journal of Research and Review*. 2023; 10(11): 504-512. DOI: <https://doi.org/10.52403/ijrr.20231158>
